

# Toward the Jamming Threshold of Sphere Packings: Tunneled Crystals

S. Torquato\*

Department of Chemistry, Princeton University, *Princeton NJ 08544*

Program in Applied and Computational Mathematics,

Princeton University, *Princeton NJ 08544*

Princeton Institute for the Science and Technology of Materials,

Princeton University, *Princeton NJ 08544 and*

Princeton Center for Theoretical Physics,

Princeton University, *Princeton NJ 08544*

F. H. Stillinger

Department of Chemistry, Princeton University, *Princeton NJ 08544*

## Abstract

We have discovered a new family of three-dimensional crystal sphere packings that are strictly jammed (i.e., mechanically stable) and yet possess an anomalously low density. This family constitutes an uncountably infinite number of crystal packings that are subpackings of the densest crystal packings and are characterized by a high concentration of self-avoiding “tunnels” (chains of vacancies) that permeate the structures. The fundamental geometric characteristics of these tunneled crystals command interest in their own right and are described here in some detail. These include the lattice vectors (that specify the packing configurations), coordination structure, Voronoi cells, and density fluctuations. The tunneled crystals are not only candidate structures for achieving the jamming threshold (lowest-density rigid packing), but may have substantially broader significance for condensed matter physics and materials science.

PACS numbers: 05.20.-y, 61.20.J, 81.05.Rm

## I. INTRODUCTION

Hard-particle models have played a substantial and insightful role in the historical development of statistical mechanics. In particular, this is true for the venerable hard-sphere model in  $d$ -dimensional Euclidean space  $\mathbb{R}^d$  in which the hyperspheres only interact with an infinite repulsion for overlapping configurations. Hard-sphere packings have provided a rich source of outstanding theoretical problems and have served as useful starting points to model the structure of granular media,<sup>1</sup> liquids,<sup>2,3</sup> glasses,<sup>3</sup> crystals,<sup>4</sup> living cells,<sup>3</sup> and random media.<sup>3</sup> Sphere packing problems have inspired scientists and mathematicians at least since the time of Kepler and continue to present open challenging problems.<sup>5,6,7,8,9</sup>

One of the perennially popular aspects of hard-sphere many-body systems concerns their “jamming” properties, i.e., their mechanically stable packing arrangements. Jamming behavior of sphere packings is intimately related to classical ground-state structures and to glassy states of matter. The present paper concentrates on one portion of that packing arrangement issue that to the best of our knowledge has not previously been explored, namely, the “strict” jamming threshold of three-dimensional sphere packings.

Three broad and mathematically precise “jamming” categories of sphere packings can be distinguished depending on the nature of their mechanical stability;<sup>10</sup> see also Ref. 11. In order of increasing stringency (stability) for a finite system of hard spheres, these are the following:

**Local jamming:** Each particle in the system is locally trapped by its neighbors, i.e., it cannot be translated while fixing the positions of all other particles.

**Collective jamming:** Any locally jammed configuration is collectively jammed if no subset of particles can simultaneously be displaced so that its members move out of contact with one another and with the remainder set. An equivalent definition is to ask that all finite subsets of particles be trapped by their neighbors.

**Strict jamming:** Any collectively jammed configuration that disallows all globally uniform volume-nonincreasing deformations of the system boundary is strictly jammed.

It is important to note that the jamming category depends on the boundary conditions employed. For example, hard-wall boundary conditions<sup>10</sup> generally yield different jamming classifications from periodic boundary conditions.<sup>12</sup> These jamming classifications are closely re-

lated to the concepts of “rigid” and “stable” packings found in the mathematics literature.<sup>13</sup> Rigorous and efficient linear-programming algorithms have been devised to assess whether a particular hard-sphere configuration is locally, collectively, or strictly jammed.<sup>12,14</sup>

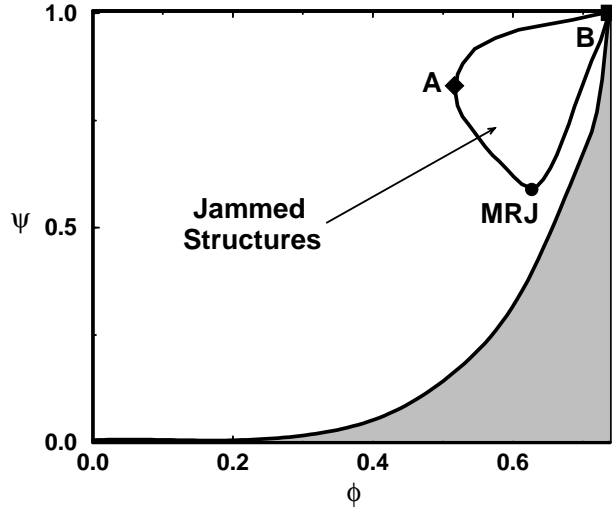


FIG. 1: A highly schematic plot of the jammed subspace in the density-disorder ( $\phi$ - $\psi$ ) plane, taken from Ref. 15. Point A corresponds to the lowest-density jammed packing, and it is intuitive to expect that a certain ordering will be needed to produce low-density jammed packings. Point B corresponds to the densest jammed packing. Point MRJ represents the maximally random jammed state, i.e., the most disordered state subject to the jamming constraint.

The enumeration and classification of both ordered and disordered jammed circular disk and sphere packings for the various jamming categories is an outstanding problem. Since one cannot enumerate all possible packings even for a small number of particles, it is desirable to devise a small set of parameters that can characterize packings well. One important property of a sphere packing is the packing fraction  $\phi$ , which is defined to be the fraction of space covered by the particles. Another useful way to characterize a packing is via scalar order metrics.<sup>3,15</sup> An order metric  $\psi$  is a well-defined scalar function of a configuration of spheres and is subject to the normalization  $0 \leq \psi \leq 1$ . For any two states  $X$  and  $Y$ ,  $\psi(X) > \psi(Y)$  implies that state  $X$  is to be considered as more ordered than state  $Y$ . Candidates for such an order metric include various translational and orientational order parameters<sup>3,15,16</sup> but the search for better order metrics is still very active. Figure 1 from Ref. 15 shows a highly

schematic region of feasible hard-sphere packings in the  $\phi$ - $\psi$  plane, which has been called an “order map.” It is clear that only a small subset of this feasible region will be occupied by jammed packings for a given jamming category, as indicated in Fig. 1. The following extremal points in the jammed region are particularly interesting:

1. Point A corresponds to the lowest-density jammed packing, i.e., the jamming threshold, and its location strongly depends on the jamming category used. We denote by  $\phi_{\min}$  the corresponding jamming-threshold packing fraction, which is expected to be characterized by a high degree of order, as discussed in more detail below. As discussed below, local jamming is a very weak condition compared to collective or strict jamming.
2. Point B corresponds to the most dense jammed packing. It has of course already been identified to be a triangular lattice packing for circular disks, and the face-centered cubic lattice packing and its stacking variants for spheres. But much less is known about polydisperse packings<sup>18,19,22</sup> or packings of nonspherical particles.<sup>23,24</sup>
3. The MRJ point represents the *maximally random jammed state*,<sup>15</sup> which has been suggested to replace the ill-defined random close packed (RCP) state.<sup>17</sup> The MRJ state is the most disordered jammed packing in a given jamming category (i.e., locally, collectively, or strictly jammed). The MRJ state is well-defined for a given jamming category and choice of order metric. The strict MRJ state can be regarded to be the *prototypical glass* – it is the most disordered packing arrangement that is able to withstand shear forces.

It is crucial to note that the *order map* shown in Fig. 1 is independent of the protocol used to generate a hard-sphere configuration. In practice, one can use a variety of protocols to produce jammed configurations in order to delineate the boundary of the jammed region shown in Fig. 1, as was partially done in Ref. 16. Moreover, the frequency of occurrence of a particular configuration is irrelevant in so far as the order map is concerned. In other words, the order map emphasizes a statistical-geometric approach to packing by characterizing single configurations regardless of their occurrence probability. Therefore, ensemble methods that inherently produce “most probable” configurations might miss interesting extremal points in the order map, such as point A.

The preponderance of work on sphere packings has been devoted to the determination of point B in Fig. 1 for low as well as high dimensions.<sup>5,8</sup> It is known that the densest arrangements of monodisperse disks in two dimensions and spheres in three dimensions are strictly jammed.<sup>10,12</sup> This implies that shear moduli of these packings are infinitely large. The densest sphere packings have a packing fraction given by

$$\phi_{\max} = \frac{\pi}{\sqrt{18}} = 0.74048\dots \quad (1)$$

It has long been known empirically that this maximum is attained both by the face-centered cubic (fcc) and the hexagonal close packed (hcp) crystal structures, as well as by their stacking hybrids. A mathematically rigorous proof of Eq. (1) has only recently appeared.<sup>8</sup>

We are interested in characterizing point A in Fig. 1 for collectively and strictly jammed packings, which has received far less attention than the determination of point B. Specifically, it is desired to identify such packing arrangements and the corresponding jamming-threshold packing fraction  $\phi_{\min}$ . It is possible to arrange hard spheres in space, subject only to the weak locally jammed criterion, so that the resulting packing fraction is arbitrarily close to zero.<sup>20,21</sup> But demanding either collective jamming or strict jamming evidently forces  $\phi$  to equal or exceed a lower limit  $\phi_{\min}$  that is well above zero. No rigorous theory or even empirical study has heretofore convincingly determined  $\phi_{\min}$  for collectively or strictly jammed monodisperse hard spheres.

The present paper is devoted to a description of a class of strictly jammed three-dimensional sphere packings with anomalously low packing fraction, substantially lower indeed than the lowest previously known result.<sup>16,21</sup> This class appears to be a new family of crystal structures. We do not know if the resulting packing fraction for this class actually attains  $\phi_{\min}$ . The packing structures involved rely on an earlier observation that linear arrays, or tunnels, of vacancies generated in close-packed crystals, even with branching, do not destroy the mechanical stability of the resulting structures.<sup>21</sup>

The following Section II provides some background on the problem and describes previous work on low-density jammed packings. Section III provides a structural characterization of the class of low- $\phi$  tunneled structures. Via application of a computational test,<sup>12,14</sup> we establish that strict jamming is attained in these structures. The final Section IV contains discussion, including the informal argument that approaching or attaining  $\phi_{\min}$  requires a regular periodic structure, not an amorphous packing.

## II. BACKGROUND AND PREVIOUS WORK

One way to reduce the density of a strictly jammed packing while retaining the strict jamming characteristic is to selectively remove subsets of spheres from the fcc, hcp, or hybrid close packed crystals. This leaves behind an array of vacancies. In this approach it is important to avoid removing triads of spheres that were in mutual contact in the starting crystal, i.e., a compact equilateral triangle of spheres, because that leads to local instability.<sup>21</sup> However, one viable option involves removing one-quarter of the spheres from an fcc crystal, specifically those that constitute one of its four simple-cubic sublattices. The result remains strictly jammed<sup>21</sup> and thus leads to the following bound:

$$\phi_{\min} \leq \frac{\pi}{2^{5/2}} = 0.55536 \dots \quad (2)$$

In addition to the vacancy-containing crystals just described, collectively and strictly jammed packings with  $\phi < \phi_{\max}$  also exist with irregular (non-periodic) sphere arrangements. Indeed, in Ref. 15 it was shown that using the Lubachevsky-Stillinger algorithm,<sup>25</sup> one can produce such packings in non-trivial range of packing fraction:

$$0.64 < \phi < 0.74048 \dots \quad (3)$$

where 0.64 corresponds to the packing fraction of the MRJ state. In fact, we have conjectured that the Lubachevsky-Stillinger packing algorithm typically produces packings along the right (maximally dense) branch from the MRJ point to the maximally dense point B in Fig. 1.<sup>26</sup> Importantly, we do not know of an algorithm that can systematically produce packings along the left (minimally dense) branch without relying on some random removal process. Indeed, it has been shown that by randomly diluting the fcc packing (subject to the constraint that no compact equilateral triangular vacancies are created), strictly jammed packings with a packing fraction of 0.52 can be created.<sup>16</sup> It should not escape notice that these considerations suggest that amorphous sphere configurations cannot attain the jamming threshold  $\phi_{\min}$ . Rather it is very plausible that  $\phi_{\min}$  is achieved by structures characterized by a large order metric  $\psi$  value, as schematically indicated in Fig. 1. In other words,  $\phi_{\min}$  is likely to be realized by crystal (i.e., periodic) packings.<sup>27</sup> Typical large, jammed packings produced via experimental as well as computer-simulation protocols are characterized by a significant degree of disorder, and therefore such protocols would never find such crystal candidates because they are sets of zero measure.

*Isostatic* packings are jammed packings that have the minimal number of contacts to maintain a particular jamming classification, a situation that are normally associated with amorphous packing such as the MRJ state (c.f. Fig. 1). In the limit of an infinitely large packing, collective and strict jamming become equivalent constraints and the corresponding isostatic condition implies an average of  $2d$  contacts per particle,<sup>26</sup> where we recall that  $d$  is the space dimension. Thus, ordered but strictly jammed sphere packings in  $\mathbb{R}^d$  with  $2d$  contacts per particle would seem to be natural candidates to achieve the jamming threshold. Indeed, in  $\mathbb{R}^2$ , the so-called “reinforced” Kagomé packing with precisely 4 contacts per particle is evidently the lowest density strictly jammed subpacking of the triangular lattice packing<sup>12,28</sup> with  $\phi_{\min} = \sqrt{3}\pi/8 = .68017\dots$ . The  $d$ -dimensional generalization of the two-dimensional Kagomé packing has exactly  $2d$  contacts per particle because each particle is the vertex of vertex-sharing simplices<sup>1</sup> and would appear to achieve the desired jamming threshold. In three dimensions, this structure is the well-known pyrochlore crystal that has received considerable attention because such material structures can exhibit exotic magnetic behavior; see Refs. 29 and 30, and references therein. The three-dimensional Kagomé packing possesses a rather low packing fraction ( $\phi = \pi/\sqrt{72} = 0.37024\dots$ ), but, unfortunately, it contains equilateral-triangle-vacancy cluster and therefore cannot be collectively or strictly jammed. Thus, the  $d$ -dimensional Kagomé packing is not strictly jammed for  $d \geq 3$ .

Note that in a Bravais lattice packing, the space  $\mathbb{R}^d$  can be geometrically divided into identical regions called *fundamental cells*, each of which contains the center of just one sphere. Non-Bravais-lattice packings include periodic packings, in which there is more than one sphere per fundamental cell, as well as disordered packings.

---

<sup>1</sup> The  $d$ -dimensional Kagomé packing contains  $d+1$  spheres per fundamental cell i.e., it has a  $(d+1)$ -particle basis. The centroids of the simplices of this structure are the sites of the  $d$ -dimensional *diamond* crystal that possesses a 2-particle basis and placing the largest nonoverlapping hypersphere at each of these sites produces the densest  $d$ -dimensional diamond packing. The “two-dimensional diamond” packing is nothing more than the “honeycomb” packing, which is the basic building block used to create the tunneled three-dimensional crystals that are the focus of this paper. Placing the largest nonoverlapping hypersphere at each of the midpoints of the “bonds” joining the sites of the  $d$ -dimensional diamond packing yields the densest  $d$ -dimensional Kagomé packing. Detailed geometrical characteristics of the latter packing for arbitrary  $d$  will be reported in a future study.

### III. TUNNELED CLOSE-PACKED SPHERE PACKINGS

We begin by reminding the reader about the elementary distinctions between the fcc, the hcp, and the hybrid close-packed structures. All can be conveniently viewed as stacks of planar triangular arrays of spheres, within which each sphere contacts six neighbors. These triangular layers can be stacked on one another, fitting spheres of one layer into "pockets" formed by nearest-neighbor triangles in the layer below. At each such layer addition there are two choices of which set of pockets in the layer below are to be filled. A lower layer with lateral position to be called A, is then surmounted with the next layer in lateral position B or C. A third layer subsequently can revert to lateral position A, or can be C on a second layer B, or B on second layer C. The fcc structure is a Bravais-lattice packing that utilizes the repeating pattern:

$$\dots \text{ABCABCABC} \dots \quad (4)$$

while the hcp case (a periodic non-Bravais-lattice packing) corresponds to:

$$\dots \text{ABABABAB} \dots \quad (5)$$

Hybrid close-packed structures utilize other A,B,C patterns of lateral positions, never immediately repeating one of these three letters. Since there are two ways to place each layer after the second, there is an uncountable infinity of distinct packing schemes, all with the same density. These are called the Barlow packings<sup>31</sup> and include *random* stacking variants (i.e., the two ways to place each layer after the second occur with equal probabilities.). In the latter case, there is no repeating pattern, as exhibited by the following partial sequence:

$$\dots \text{ABACBACBCA} \dots \quad (6)$$

The tunneled crystal structures to which this paper is devoted can similarly be classified by a layer lateral displacement A,B,C code. However, the constituent planar layers to be stacked are not triangular, but have the lower density "honeycomb" pattern. The latter is illustrated in Fig. 2. This amounts to the preceding triangular layer with one-third of its spheres removed in a periodic pattern. Each remaining sphere in the honeycomb layer contacts three neighbors in that layer. A periodic primitive or fundamental cell for the honeycomb structure in two dimensions contains two spheres, not just one as for the triangular-lattice layer.



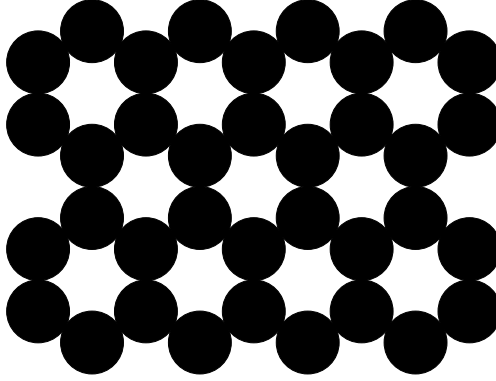


FIG. 2: A portion of a honeycomb layer structure.

By adapting the three jamming category definitions to two dimensions, one immediately discovers that the honeycomb structure by itself is only locally jammed.<sup>10</sup> It is easy to see from Fig. 2 that the set of six particles surrounding any vacancy can be rotated as a unit about its center to eliminate six contacts within the layer. Repetition of this process, along with other subsequently allowed displacements, would totally un-jam the layer. However, this intra-layer instability is eliminated when honeycomb layers are placed one upon another, following one of the previously-described A,B,C codes. Note that there are three different choices for the direction of the tunnels at each stacking stage. There are an uncountably infinite number of such stacking arrangements that we refer to as the “tunneled” crystals.

### A. Tunneled FCC Crystal

Consider first the fcc code (4), which is depicted in the left panel of Fig. 3. The right panel is a photograph of a corresponding ball-bearing construction, which shows the manifest stability of the packing. The periodic result in three dimensions has a fundamental cell containing two spheres. Assuming that the spheres have unit diameter, the basis vectors locating sphere centers for the fundamental cell can be assigned as follows:

$$\mathbf{a}_1 = \sqrt{3}\mathbf{i}, \quad \mathbf{a}_2 = -\frac{\sqrt{3}}{2}\mathbf{i} + \frac{3}{2}\mathbf{j}, \quad \mathbf{a}_3 = -\frac{\sqrt{3}}{6}\mathbf{i} + \frac{1}{2}\mathbf{j} + \frac{\sqrt{2}}{3}\mathbf{k}. \quad (7)$$

The additional sphere in this fundamental cell is located at

$$\mathbf{b}_1 = \mathbf{j}. \quad (8)$$

As a result of using honeycomb layers to form this structure, the packing fraction is

$$\phi = \frac{2}{3}\phi_{\text{max}} = \frac{\sqrt{2}\pi}{9} = 0.49365 \dots \quad (9)$$

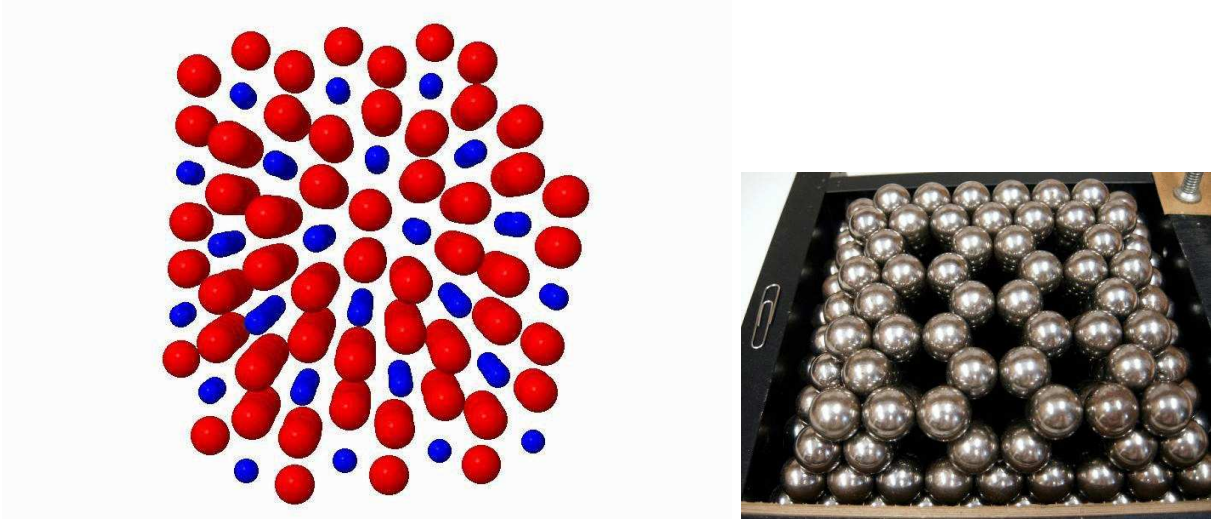


FIG. 3: Left panel: A view of the “tunneled” fcc crystal looking along the axis perpendicular to the honeycomb layers. The vacancies are shown as smaller red particles and the actual particles are colored blue. The “tunnels” consist of linear chains of vacancies and are parallel to one another. Right panel: A photograph of the tunneled fcc crystal built up from ball bearings of diameter 5/8 inches. This actual construction shows the manifest stability of the tunneled fcc crystal.

Examination of the tunneled fcc crystal structure reveals that it contains a periodic array of parallel linear tunnels. The direction of these tunnels is that of cube-face diagonals for the parent fcc crystal. By symmetry this tunnel array could have been oriented in any one of six equivalent directions. Each remaining sphere in the tunneled fcc crystal lies immediately next to three tunnels. The number of neighbor contacts experienced by each sphere is seven, comprising three within its own honeycomb layer, and two each from the honeycomb layers immediately below and above. The spatial arrangement of these seven contacting neighbors is chiral (i.e., the mirror image of one is not superimposable on the other), with equal numbers of left- and right-handed versions present (see Fig. 4). Clearly, the tunneled fcc crystal has a lower symmetry than its parent unvacated fcc packing.



FIG. 4: The chiral pairs of seven contacting neighbor arrangements in the tunneled fcc packing. The orientation of the three red spheres that contact a central blue sphere within each honeycomb layer is the same in both chiral alternatives.

Associated with each sphere center is its *Voronoi cell*, which is defined to be the region of space nearer to this center than to any other sphere center. The Voronoi cells for any general point process are convex polyhedra whose interiors are disjoint, but share common faces, and therefore the union of all of the polyhedra tiles the space. Not surprisingly, there are two types of Voronoi cells for the tunneled fcc packing, one being the mirror image of the other (see Fig. 5) and therefore, since these cells cannot be superimposed on one another, they are chiral pairs. The volume of each Voronoi cell is  $3/2$  times the volume of the Voronoi cell (rhombic dodecahedron) of an unvacated fcc packing.

The vector  $\mathbf{R} = n_1\mathbf{a}_1 + n_2\mathbf{a}_2 + n_3\mathbf{a}_3 + n_4\mathbf{b}_1$  spans all of the sphere centers in the tunneled fcc crystal, where the vectors  $\mathbf{a}_i$  and  $\mathbf{b}_1$  are defined by (7) and (8), respectively, the  $n_i$  are the integers, and  $n_4 = 0$  or  $1$ . Thus, the corresponding squared distance from the origin is given by

$$R^2 = 3(n_1^2 + n_2^2 - n_1n_2 + n_2n_4) + 2n_2n_3 + n_3^2 + n_4^2 + n_3n_4 - n_1n_3. \quad (10)$$

The quadratic form (10) enabled us to determine the theta series  $\theta_{tfcc}(q)$  for the tunneled fcc crystal up to an arbitrarily large number of terms (100,000 or more). The first 14 terms of this series are given by

$$\theta_{tfcc} = 1 + 7q + 4q^2 + 18q^3 + 7q^4 + 16q^5 + 6q^6 + 28q^7 + 4q^8 + 30q^9 + 14q^{10} + 16q^{11} + 18q^{12} + 42q^{13} + \dots \quad (11)$$

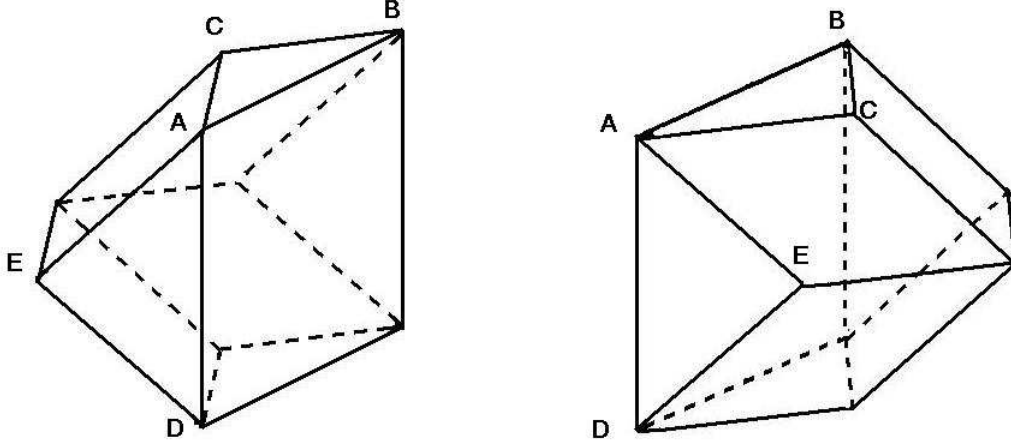


FIG. 5: The chiral pairs of Voronoi cells in the tunneled fcc packing. Each cell has 9 faces: one rectangular face (with side lengths of 1 and  $3/2$ ), two isosceles triangular faces (with side lengths 1 and  $1/\sqrt{2}$ ), two other isosceles triangular faces (with side lengths  $3/2$  and  $1/\sqrt{2}$ ), and four rhombical faces (with side lengths  $3/2$  and  $1/\sqrt{2}$ ). The edge lengths indicated are given as follows:  $\overline{AB} = 1$ ,  $\overline{AC} = 1/\sqrt{2}$ ,  $\overline{BC} = 1/\sqrt{2}$ ,  $\overline{AD} = 3/2$ ,  $\overline{AE} = 1/\sqrt{2}$ , and  $\overline{DE} = 1/\sqrt{2}$ . Each cell has 16 edges and 9 vertices. Merging the two rectangular faces (mirror planes) so that they coincide results in a dodecahedron (12-faced polyhedron) that tiles the space.

The theta series is a fundamental characteristic of a packing that encodes coordination structure information,<sup>5</sup> namely, the exponent of  $q$  gives the squared distance of spheres from a sphere located at the origin and the associated coefficient is the number of spheres located at that squared distance. The result (11) should be contrasted with the corresponding theta series for the unvacated fcc packing given by

$$\theta_{fcc} = 1 + 12q + 6q^2 + 24q^3 + 12q^4 + 24q^5 + 8q^6 + 48q^7 + 6q^8 + 36q^9 + 24q^{10} + 24q^{11} + 24q^{12} + 72q^{13} + \dots \quad (12)$$

Observe that the coordination shell distances are the same for both the tunneled fcc crystal and its saturated counterpart, but the corresponding occupation numbers in the former are always strictly less than those in the latter. This strict bound is true for every coordination shell.

We note in passing that the corresponding three-dimensional crystals formed by stacking Kagomé layers can be obtained from the honeycomb-stacking arrangements by placing the largest nonoverlapping sphere at each of the midpoints of the bonds joining the spheres in

each honeycomb layer (as per the  $d$ -dimensional mapping described in the footnote.) The Kagomé stackings have a packing fraction (i.e., three fourths of  $\phi_{\max}$ ) that is considerably higher than that of the honeycomb stackings, and a contact number of 8.

## B. Tunneled HCP Crystal

The alternative layer stacking code (5) that is associated with the hcp crystal also produces a regular tunnel array, exhibiting the same packing fraction (9). However, in this case the tunnels have a zig-zag shape with overall orientation parallel to the hexagonal “c” direction. The zig-zag tunnels have three possible lateral directional orientations, depending on whether the constituent honeycomb layers were stacked periodically as AB, AC, or BC pairs. These choices have the zig-zags rotated relative to one another by plus or minus 60 degrees, when viewed down the hexagonal c axis. Once again the spheres have seven contacts with immediate neighbors, but those seven neighbors have a non-chiral arrangement. Similarly, in contrast to the tunneled fcc packing, the hcp counterpart has a unique Voronoi cell, even if it is substantially less symmetrical than the ones depicted in Fig. 5. The former also possesses 16 edges and 9 vertices as well as 9 faces: two irregular quadrilaterals, two pairs of irregular triangles, and three quadrilaterals, each with a mirror axis of symmetry. Of course, the volume of the cell is 3/2 times the volume of an unvacated hcp packing.

The tunneled hcp crystal has a fundamental cell containing three spheres. Again, assuming that the spheres have unit diameter, the basis vectors locating sphere centers for the fundamental cell can be designated as follows:

$$\mathbf{a}_1 = \sqrt{3}\mathbf{i}, \quad \mathbf{a}_2 = -\frac{\sqrt{3}}{2}\mathbf{i} + \frac{3}{2}\mathbf{j}, \quad \mathbf{a}_3 = \frac{\sqrt{8}}{3}\mathbf{k}. \quad (13)$$

The additional two spheres in this fundamental cell are located at

$$\mathbf{b}_1 = \mathbf{j}, \quad \mathbf{b}_2 = -\frac{\sqrt{3}}{6}\mathbf{i} + \frac{1}{2}\mathbf{j} + \frac{\sqrt{2}}{3}\mathbf{k}. \quad (14)$$

The vector  $\mathbf{R} = n_1\mathbf{a}_1 + n_2\mathbf{a}_2 + n_3\mathbf{a}_3 + n_4\mathbf{b}_1 + n_5\mathbf{b}_2$  spans all of the spheres in the tunneled hcp crystal, where the vectors  $\mathbf{a}_i$  and  $\mathbf{b}_i$  are defined by (13) and (14), respectively, the  $n_i$  are the integers,  $n_4 = 0$  or 1, and  $n_5 = 0$  or 1. The corresponding squared distance from the origin is given by

$$R^2 = 3(n_1^2 + n_2^2 - n_1n_2 + n_2n_5) + 2n_2n_5 + n_4^2 + n_5^2 + n_4n_5 - n_1n_5 + \frac{8}{3}n_3^2 + \frac{8}{3}n_3n_5. \quad (15)$$

The theta series  $\theta_{thcp}(q)$  for the tunneled hcp crystal was also determined up to 10,000 terms or more. The first 14 terms of this series are

$$\theta_{thcp} = 1 + 7q + 4q^2 + 2q^{8/3} + 14q^3 + 6q^{11/3} + 3q^4 + 8q^5 + 12q^{17/3} + 4q^6 + 4q^{19/3} + 6q^{20/3} + 14q^7 + 4q^{22/3} + \dots \quad (16)$$

The result (16) should be contrasted with the theta series for the unvacated hcp packing given by

$$\theta_{hcp} = 1 + 12q + 6q^2 + 2q^{8/3} + 18q^3 + 12q^{11/3} + 6q^4 + 12q^5 + 12q^{17/3} + 6q^6 + 6q^{19/3} + 12q^{20/3} + 24q^7 + 6q^{22/3} + \dots \quad (17)$$

Although the coordination shell distances are the same for both the tunneled hcp crystal and its saturated counterpart, the corresponding occupation numbers in the former are always less or equal to those in the latter. The fact that the occupation numbers in the tunneled hcp and unvacated hcp packings can sometimes be identical never occurs in the fcc analogs.

### C. Tunneled Barlow Packings

Associated with the infinite number of Barlow packings are the infinite number of tunneled Barlow packings that are obtained by stacking the honeycomb layers (two of which are the tunneled fcc and hcp crystals). However, this infinite set of packings is larger than the unvacated Barlow packings because, as noted earlier, there are three different choices for the direction of the tunnels at each stacking stage. Of course, all of the tunneled Barlow packings have the packing fraction specified by (9).

At first glance, the tunneled packings may seem to be similar in structure to crystal structures involving honeycomb stackings found in nature, such as hexagonal graphite and boron nitride.<sup>32</sup> However, the locations of the honeycomb layers relative to one another are distinctly different in the latter and, in particular, are not sublattices of the unvacated Barlow packings.

### D. Computer Tests of Jamming Category

In earlier work,<sup>10</sup> we suggested that the aforementioned jamming categories can be tested using numerical algorithms that analyze an equivalent contact network of the packing under

applied displacements. Subsequently, a rigorous but practical algorithm was devised to assess the jamming category of a sphere packing in this fashion.<sup>12,14</sup> The algorithm is based on linear programming and is applicable to regular as well as random packings of finite size with hard-wall and periodic boundary conditions. If the packing is not jammed, the algorithm yields representative multi-particle unjamming motions.

We begin by testing the tunneled fcc crystal using this algorithm. The fundamental (primitive) cell is replicated to form a periodic unit cell with  $N$  spheres, i.e., to form a finite periodic packing. It turns out that the tunneled fcc crystal for any finite  $N$  under periodic boundary conditions structures is not collectively jammed. (The actual  $N$  used was as large as 500.) Although each sphere possesses 7 contacting particles, the 2 contacting particles below and above the plane containing the central sphere [cf. (Fig. 4)] can move collectively, enabling the central sphere to roll into the tunnels. This causes unjamming of the entire packing. However, if one replaces a single honeycomb layer of the tunneled crystal structure at one of the boundaries of the unit cell with a perfect triangular-lattice layer of spheres, the aforementioned collective motion is eliminated and the packing is strictly jammed. This surface triangular-lattice layer of particles does not contribute to the density in the infinite-packing limit, and, therefore, the jamming threshold is given by (9). This reinforcement by a single triangular-lattice layer is also the reason for the stability of the ball-bearing construction depicted in Fig. 3. The tunneled hcp crystal packing also has an instability without reinforcement, but becomes strictly jammed by inserting a perfect triangular-lattice layer of particles in the manner described above.

Based on these results, it can be argued that any stacking variant of the honeycomb layers will also be strictly jammed when reinforced by a triangular-lattice layer. Indeed, in computer tests for random honeycomb stackings with up to 1000 spheres per periodic unit cell, strict jamming is achieved.

### E. Hyperuniformity

An important characteristic of a packing is the extent to which long-wavelength density fluctuations are suppressed. A *hyperuniform* point pattern is one in which infinite-wavelength density fluctuations vanish identically.<sup>33</sup> This property implies that the number variance of sphere centers within a compact subregion of space (window) grows more slowly

than the volume of the window. All periodic packings are *hyperuniform*.<sup>33</sup> However, not all packings that are hyperuniform are necessarily rigid in the sense of strict jamming,<sup>11</sup> especially if they are not saturated. A packing is *saturated* if there is no space available to add another sphere without overlapping the existing particles. Thus, both the tunneled fcc and hcp crystals are unusual packings in that they are hyperuniform (because they are periodic) and strictly jammed (despite the fact that they are unsaturated). It appears that the property of hyperuniformity extends to all of the tunneled Barlow packings, including the purely disordered ones. The reason is that any single honeycomb layer is itself hyperuniform and translations of the honeycomb layers in the *equally spaced* honeycomb planes in the stacked arrangements should not accumulate long-wavelength density fluctuations. A rigorous proof that the tunneled random stacking variant is hyperuniform would require one to show that the structure factor vanishes in the limit of vanishing wavenumber using the methods of Ref. 11 that were applied to other crystal structures.

#### IV. DISCUSSION AND CONCLUSIONS

Beside their intrinsic relevance for hard-sphere-jamming phenomena, the existence of tunneled crystal structures may have substantially broader significance for solid state physics and materials science. For example, the directionality of the parallel arrays of tunnels in the tunneled fcc packing (described in Sec. III) might produce some unusual properties that exploit the resulting anisotropy. One obvious candidate, say for the linear tunnels in the fcc-parent case, would be separation technology for substances whose constituent particles have just the right size to diffuse along those tunnels, leaving behind larger impurity particles. In the event that a metallic element or alloy were to be rendered in the form of a tunneled crystal, the electronic characteristics would doubtless be strongly influenced by the structural anisotropy. The anisotropic porosities of a tunneled crystal also suggest that they might serve as catalytic substances for reactants that fit into these pores. Elsewhere, the magnetic properties of the tunneled crystals are being studied by examining the classical Heisenberg Hamiltonian for Ising, XY, and Heisenberg spins on these structures.<sup>35</sup>

It should be kept in mind that the tunneled crystal structures conceivably could be synthesized at the atomic scale, or alternatively at a larger length scale they might be assembled from spherical colloids. In such instances, the mechanical stability of the crystals



could be enhanced via attractive interactions that are absent in the sphere packings. In the case of colloids, the attractive interactions can be optimized for mechanical stability using inverse statistical-mechanical techniques; see Ref. 34 and references therein.

As stressed earlier, we have no proof that the tunneled-crystal packing fraction shown in Eq. (9) is the lowest attainable for collectively or strictly jammed sphere packings. It is noteworthy that any attempt to remove even a single additional sphere from the tunneled fcc, hcp, or hybrid tunneled crystals immediately causes the structure to begin collapsing. However, this observation does not in itself eliminate the possibility of discovering some other unrelated class of structures with yet a smaller packing fraction  $\phi$ . One might suspect that if such a lower density structure were to be created, it might exhibit a number of contacts per sphere less than the seven present in all of the cases described herein. As we noted earlier, isostatic packings have the minimum average number of contacts of six that would be consistent with collective or strict jamming, a situation that is usually associated with the amorphous MRJ state. This disordered packing, however, has a distribution of contact numbers that in principle could be as large as the maximum value of twelve. Ulam conjectured that the maximal density for packing congruent spheres is smaller than that for any other convex body (Martin Gardner, private communication; see also ref. 32). If the tunneled crystals identified in this paper are indeed the ones that achieve the strict jamming threshold, then it may be possible that  $\phi_{\min}$  is itself minimized by spherical packing elements among all congruent convex bodies. It is also possible that the tunneled crystals provide the lowest density strictly jammed structures that are subpackings of the densest sphere packings, but that true jamming threshold is achieved by packings that are not subpackings of the densest packings.

At least in one, two, and three dimensions, the maximal density  $\phi_{\max}$  can only be attained by restricting local sphere coordination geometries to a very limited set. The result is that these maximal-density structures exhibit periodic long-range order. This is true even of the hybrid close-packed crystals, which are only partially disordered in their density distributions. By contrast, the local coordination geometries present in amorphous sphere packings are very numerous, but are overwhelmingly unsuited as structural elements for attaining  $\phi_{\max}$ . We conjecture that an analogous situation applies for the jamming threshold  $\phi_{\min}$ . The vast majority of amorphous packing coordination geometries are likewise unsuited for producing the lowest density collectively or strictly jammed sphere packings. Only

crystalline structures in three dimensions should be expected to exhibit  $\phi_{\min}$ . Whether the tunneled crystals described in this paper are the solution to this minimization remains to be seen.

The authors thank Fiona Burnell and Shivaji Sondhi for enlightening discussions concerning the magnetic properties of the tunneled crystals. We are also grateful to Yang Jiao for running the program that tests for jamming on the tunneled crystals and for creating the bulk of the figures for this paper. This work supported by the National Science Foundation under Grant No. DMS-0312067.

---

\* Electronic address: torquato@electron.princeton.edu

- <sup>1</sup> S. F. Edwards and D. V. Grinev, *Chem. Eng. Sci.* **56**, 5451 (2001).
- <sup>2</sup> J. P. Hansen and I. R. McDonald, *Theory of Simple Liquids* (Academic Press, New York, 1986).
- <sup>3</sup> S. Torquato, *Random Heterogeneous Materials: Microstructure and Macroscopic Properties* (Springer-Verlag, New York, 2002).
- <sup>4</sup> P. M. Chaikin and T. C. Lubensky, *Principles of Condensed Matter Physics* (Cambridge University Press, New York, 1995).
- <sup>5</sup> J. H. Conway and N. J. A. Sloane, *Sphere Packings, Lattices and Groups* (Springer, New York, 1998).
- <sup>6</sup> T. Aste and D. Weaire, *The Pursuit of Perfect Packing* (Institute of Physics, Bristol, 2000).
- <sup>7</sup> H. Cohn and N. Elkies, *Ann. Math.* **157**, 689 (2003).
- <sup>8</sup> T. C. Hales, *Ann. Math.* **162**, 1065 (2005).
- <sup>9</sup> S. Torquato and F. H. Stillinger, *Experimental Math.* **15**, 307 (2006).
- <sup>10</sup> S. Torquato and F. H. Stillinger, *J. Phys. Chem. B* **105**, 11849 (2001).
- <sup>11</sup> S. Torquato, A. Donev, F. H. Stillinger, *Int. J. Solids Struct.* **40**, 7143 (2003).
- <sup>12</sup> A. Donev, S. Torquato, F. H. Stillinger and R. Connelly, *J. Appl. Phys.* **95**, 989 (2004).
- <sup>13</sup> R. Connelly, K. Bezdek and A. Bezdek, *Discrete Comput. Geom.* **20**, 111 (1998).
- <sup>14</sup> A. Donev, S. Torquato, F. H. Stillinger and R. Connelly, *J. Comput. Phys.* **197**, 139 (2004).
- <sup>15</sup> S. Torquato, T. M. Truskett and P. G. Debenedetti, *Phys. Rev. Lett.* **84**, 2064 (2000).
- <sup>16</sup> A. R. Kansal, S. Torquato and F. H. Stillinger, *Phys. Rev. E* **66**, 041109 (2002).
- <sup>17</sup> As the name implies, the RCP state is traditionally thought of as the highest density that a

large random packing of spheres can attain. Besides the important fact that randomness was never quantified, it was shown that one can create packings that are progressively denser by decreasing the degree of order, and hence the concept of the RCP state is ill-defined. See Refs. 3 and 15 for further details.

- <sup>18</sup> A. R. Kansal, S. Torquato and F. H. Stillinger, *J. Chem. Phys.* **117**, 8212 (2002).
- <sup>19</sup> O. U. Uche, F. H. Stillinger, S. Torquato, *Physica A* **342**, 428 (2004).
- <sup>20</sup> K. Böröczky, *Ann. Univ. Sci. Budapest. Estvss Sect. Math.* **7**, 79 (1964)
- <sup>21</sup> F. H. Stillinger, H. Sakai and S. Torquato, *Phys. Rev. E* **67**, 031107 (2003).
- <sup>22</sup> L. Fejes-Tóth, *Regular Figures* (Pergamon, New York, 1964).
- <sup>23</sup> A. Donev, F. H. Stillinger, P. M. Chaikin and S. Torquato, *Phys. Rev. Lett.* **92**, 255506 (2004).
- <sup>24</sup> J. H. Conway, and S. Torquato, *Proc. Nat. Acad. Sci.* **103**, 10612 (2006).
- <sup>25</sup> B. D. Lubachevsky and F. H. Stillinger, *J. Stat. Phys.* **60**, 561 (1990).
- <sup>26</sup> A. Donev, S. Torquato and F. H. Stillinger, *Phys. Rev. E* **71**, 011105 (2005).
- <sup>27</sup> Any useful order metric will not assign a value of unity (perfect order) to all periodic packings, but rather assign a value generally less than unity to each according its symmetry, vacancy distribution, etc. This has been shown to be the case in practice.<sup>15,16</sup> Therefore, since we expect that the jamming-threshold structures are periodic, point A in Fig. 1 will likely have a large value of  $\psi$  but less than unity.
- <sup>28</sup> A. Donev, Ph.D. Dissertation (Princeton University, Princeton, New Jersey, 2006).
- <sup>29</sup> P. W. Anderson, *Phys. Rev.* **102**, 1008 (1956).
- <sup>30</sup> A. P. Ramirez, A. Hayashi, R. J. Cava, R. Siddharthan and B. S. Shastry, *Nature* **399**, 333 (1999).
- <sup>31</sup> W. Barlow, *Nature* **29**, 186 (1883).
- <sup>32</sup> L. Pauling, *Proc. Nat. Acad. Sci.* **56**, 1646 (1966).
- <sup>33</sup> S. Torquato and F. H. Stillinger, *Phys. Rev. E* **68**, 041113 (2003); *ibid.*, **68**, 069901 (2003).
- <sup>34</sup> M. C. Rechtsman, F. H. Stillinger and S. Torquato, *Phys. Rev. E* **75**, 031403 (2007).
- <sup>35</sup> F. Burnell and S. L. Sondhi, in preparation.
- <sup>36</sup> M. Gardner, *The Colossal Book of Mathematics: Classic Puzzles, Paradoxes, and Problems* (Norton, New York, 2001), p. 135.